This paper appears in IEEE Transactions on Systems, Man, and Cybernetics: Systems, 2017.
https://doi.org/10.1109/TSMC.2017.2738670

Haptic Tele-driving of Wheeled Mobile Robots under Non-ideal Wheel Rolling, Kinematic Control and Communication Time Delay

Weihua Li, Liang Ding, Haibo Gao and Mahdi Tavakoli, *Member, IEEE*

***Abstract*—The increasing application of WMR (Wheeled Mobile Robots) in many fields has brought new challenges on its control and teleoperation, two of which are induced by contact slippage phenomenon between wheel and terrain as well as time delays in the master-slave communication channel. In the WMR bilateral tele-driving system, in this paper, the linear velocity of the slave mobile robot follows the position command from the haptic master robot while the slippage-induced velocity error is fed back as a haptic force felt by the human operator. To cope with the slippage-induced non-passivity and constant time delays, this paper proposes three methods to design the WMR bilateral teleoperation system's controller. An experiment system is set up with Phantom Premium 1.5A haptic device as the master robot and a simulation platform of WMR as the slave robot. Experiments with the proposed methods demonstrate that they can result in a stable WMR bilateral tele-driving system under wheel's slippage and constant time-delays.**

Index Terms—kinematic control, longitudinal slippage, teleoperation, time delay, wheeled mobile robots.

I. Introduction

In recent years, the increasing interest in wheeled mobile robots (WMR)-based planetary exploration has attracted much attention to the contact slippage phenomenon between wheel and terrain, which can induce a linear velocity difference for the base of the WMR comparing with its desired input commands [1-5]. The existing slippage has brought new challenges for the WMR haptic bilateral teleoperation, which is rarely treated by researchers. In this paper, we will research the WMR bilateral teleoperation with a constant time-delay and wheel's existing slippage. It's known that the time delay existing in communication channel can not only degrade the operator's performance, but also destabilize the tele-robotic systems as the communication channel is non-passive even in the presence of small time delays [6, 7]. Especially, in the field of space exploration [8-10], the bilateral teleoperation control with time delays has been widely applied [11, 12]. Many control algorithms have been proposed in order to compensate for the time delay's influence in a teleoperation system by the researchers [13-16], most of which are developed from the perspective of passivity. Based on the passivity theory, Anderson and Spong [14] proposed scattering schemes, and Neimeyer and Slotine proposed the wave transformation algorithms for the two-port network [15, 16].

In terms of WMR's bilateral teleoperation, two kinematics-related challenges exist compared with the teleoperation of the other kinds of robots [17]: one is the mismatched workspace (the master's workspace is always restricted while the slave WMR's is relatively unlimited) [18-20]; another challenge is caused by non-holonomic constraints that limit the directions of WMR permissible motions [21]. Generally, the above are studied with the ideal assumption of wheel's pure rolling (no slippage); although many works have been done in terms of WMR tele-driving, its teleoperation on a slippery terrain with slippage is rarely involved. In this paper, the *workspace mismatch*, *surface slippage* and the *constant time delay* will be tackled simultaneously in the WMR bilateral teleoperation system. Since we consider a two-wheeled mobile robot that travels linearly without any rotation, non-holonomic constraints are not applied in this paper, which has been discussed in the previous research [22].

In our previous research [22, 23], we have shown that wheel-terrain interaction induced by the slippage can be modeled as environment termination (ET) of the slave WMR in a bilateral tele-driving system. Interestingly, we revealed that the slippage fluctuations can potentially induce the ET to present a non-passive behavior, which can destabilize the WMR teleoperation system. To overcome the communication delay, wave transformations are utilized. Different stability analyses are then conducted for the closed-loop teleoperation system.

The rest of this paper is organized as follows: In Sec. II, the WMR's kinematic model in case of a slippage, which acts as the slave robot, is presented, and a one-DOF (Degree of

This work was supported by the National Natural Science Foundation of China (51275106/61370033), Foundation for Innovative Research Groups of the National Natural Science Foundation of China (51521003), the Fundamental Research Funds for the Central Universities (HIT. NSRIF. 201705), the Natural Sciences and Engineering Research Council (NSERC) of Canada under grant RGPIN 372042-09, and the Canada Foundation for Innovation (CFI) under grant LOF 28241.

W. Li is with the School of Automotive Engineering, Harbin Institute of Technology (Weihai), Weihai, China (e-mail: liweihua.08301@163.com)

W. Li, L. Ding and H. Gao are with the State Key Laboratory of Robotics and System, Harbin Institute of Technology, Harbin, China. (phone: 0086 451 8640 2037; fax: 0086 451 8641 3857; e-mails: {liangding, gaohaibo}@hit.edu.cn)

M. Tavakoli is with the Department of Electrical and Computer Engineering, University of Alberta, Edmonton, Alberta, Canada (phone: 001 780 492 8935; e-mail: mahdi.tavakoli@ualberta.ca)

Freedom) joint robot is introduced as the master robot. In Sec. III, three methods are proposed to design the WMR bilateral tele-driving system in the presence of ET's non-passivity and constant time delays. In Sec. IV, experiments of the proposed methods are done to validate the closed-loop tele-driving system's stability and performance under a constant time-delay. Sec. V gives the concluding remarks and future work.

II. Tele-driving of a WMR with Slippage

A. WMR's Kinematic Model with Slippage

In this paper, a two-wheel actuated mobile robot is researched as Fig. 1(a) shows. Two back wheels are driven respectively by two motors and the front wheel is free of motion. It is assumed that the WMR has no rotation and, therefore, WMR's non-holonomic constraints are not considered here. While the WMR is moving on a soft/soil terrain, due to the limited friction forces and possible opposing external forces, the wheel's linear velocity v is no longer equal to the wheel's angular velocity ω times the wheel's radius r. Instead, longitudinal slippage S appears at the surface between the wheel and the terrain [5]:

$$S = \begin{cases} (r\omega - v)/v & (\omega \neq 0) \\ 0 & (\omega = 0) \end{cases}. \tag{1}$$

Here, it means that the WMR is stuck and uncontrollable in practice if v=0 and $\omega \neq 0$, which is not considered in this paper. Therefore, this paper mainly deals with the cases with a continuous fluctuating slippage as the upper equation in (1) shows.

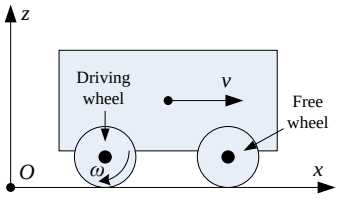

(a) A two-wheeled WMR.

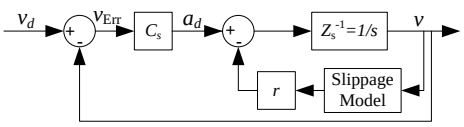

(b) Simplified WMR's kinematic model with slippage.

Fig. 1. WMR's kinematic model and control with slippage.

As a result, the traditional embedded motor's angular velocity controller cannot present good tracking performance for the WMR's velocity under wheel's slippage influence. In [22], an *embedded angular acceleration-level* controller for the motors is proposed and presented as shown in Fig. 1(b), which works to compensating for the difference (v_{Err}) of the command velocity (v_d) and the actual velocity (v) for the WMR. Here, a unity transfer function from $\dot{\omega}_d$ to $\dot{\omega}$ is assumed in kinematics. The WMR kinematic model in the presence of slippage is given as (2), which connects the wheel's angular acceleration and the WMR's linear acceleration. By differentiating $Sv = r\omega - v$ obtained from (1) as [22] did, we can obtain

$$r\left(\dot{\omega} - \underbrace{\frac{1}{r}\left(S\dot{v} + \dot{S}v\right)}_{\text{slippage model}}\right) = \dot{v}. \tag{2}$$

Note that S and $\dot{S}$ are both time-varying functions.

In Fig. 1(b), a_d is a desired linear acceleration for the WMR decided by the linear velocity error, which is then transferred to the motor's angular acceleration-level controller. The detailed explanation can be referred in the reference [22].

B. Slave Robot's Model

From the definition of the wheel's slippage in (1), the slippage looks only to be influenced by the WMR's states including the WMR's linear velocity and wheel's angular velocity. In practice, the generated slippage magnitude on a soft terrain is not decided by these states, but mostly by the WMR/terrain interaction's characteristics. With the WMR in *Part A* acting as a slave robot of a bilateral teleoperation system, the wheel/terrain interaction decided by the terrain-dependent slippage can be modeled as the "environment termination" (ET) with which the slave robot interacts.

Defining the slave WMR's linear velocity v_s, the control input $u_s = a_d$ and the environment interaction force δ_e, by means of (2), the kinematic model of the slave WMR under a slippage case can be given as

$$\dot{v}_s = u_s - \delta_e, \tag{3}$$

where $\delta_e(t) = S(t)\dot{v}_s(t) + \dot{S}(t)v_s(t)$.

Here, we only care about the case of $r\omega > v$ in (1), corresponding to $S > 0$, which means that the slippage causes a *reduction* on the WMR's linear velocity. It is also assumed that the slippage's changing rate is limited with $\dot{S}_L < \dot{S} < \dot{S}_U$, where $\dot{S}_L$ and $\dot{S}_U$ are practically decided by the wheel's states and the WMR/terrain contact characteristics.

Equation (3) provides a simplified model of the WMR with slippage as a slave robot interacting with a soft terrain. In (3), the environment interaction δ_e is assumed to be an equivalent external force applied on the WMR, and represents a generalization of the terrain-dependent slippage-induced force. Our previous research [22] has given the following property to determine the degree of the activity of the ET sub-system in (3).

Property 1 The environment termination in (3), when $\dot{S}$ is negative, is input non-passive (INP) with a shortage of passivity (SOP) of $-0.5\dot{S}_L$.

Proof: With the input $v_s(t)$ and the output $\delta_e(t)$, the ET sub-system in (3) satisfies the following inequality for all $v_s(t)$ and $T \geq 0$:

$$\begin{aligned} \int_0^T \delta_e(t)v_s(t)dt &= \int_0^T v_s(t)\left(S(t)\dot{v}_s(t) + \dot{S}(t)v_s(t)\right)dt \\ &= \underbrace{V(T) - V(0)}_{Z_{e1}} + \underbrace{\frac{1}{2}\int_0^T \dot{S}(t)v_s(t)v_s(t)dt}_{Z_{e2}} \\ &\geq -V(0) + \underbrace{\frac{1}{2}\dot{S}_L}_{\text{SOP}}\int_0^T v_s(t)v_s(t)dt, \end{aligned} \tag{4}$$

where $V(t)=\frac{1}{2}S(t)v_s^2(t)\geq 0$ since it is assumed that $S(t)>0$. Equation (4) shows that the ET is an INP system with a worst SOP of $-0.5\dot{S}_L$ [32, 34], when $\dot{S}$ is negative.

C. Master Robot's Model

In this paper, a one-DOF robot is considered as the master robot, whose dynamics can be described as

$$M_m\ddot{q}_m+B_m\dot{q}_m=\tau_m+\tau_h, \tag{5}$$

where, M_m and B_m are the robot's mass and damping coefficient, q_m is the joint position of the robot, τ_m and τ_h are the torques respectively acted by the motor and the human operator.

In the traditional non-mobile robot bilateral teleoperation systems, the velocities and/or positions of the master robot and the slave robot are always synchronized. As the above analysis, due to the WMR's unlimited workspace, while tele-driving a WMR, the DOF's mapping between the master's position q_m and the slave's velocity v_s is more appropriate. Following the works [17, 22], a new variable $r_m=\lambda\dot{q}_m+q_m$ $(0<\lambda<1)$ is used instead of $\dot{q}_m$ as a velocity command; then, the problem will require coordinating r_m and v_s (the scaling factor is set as 1). Obviously, when λ and/or $\dot{q}_m$ is small enough, an approximate mapping of position-velocity ($q_m\approx v_s$) can be achieved.

In order to map r_m and v_s, the motor's controller τ_m in (5) is designed as $\tau_m=\tau_m^*+\bar{\tau}_m$, which consists of a local controller τ_m^* and a term $\bar{\tau}_m$ that will be discussed in Sec. III. Following the previous work in [22], the local controller is designed as $\tau_m^*=-B_{Lv}\dot{q}_m$ in this paper, so that the master robot's dynamic model (5) becomes as (6) with r_m as system state

$$\bar{M}_m\dot{r}_m=\bar{\tau}_m+\tau_h, \tag{6}$$

where $\bar{M}_m=M_m/\lambda$, and $B_{Lv}=\frac{M_m}{\lambda}-B_m$.

As [17, 22, 31] presented, the human operator has the ability to adjust his/her impedance to guarantee the human termination's passivity when it is augmented with the above introduced position/velocity mapping. In practice, the human operator can automatically regulate the relaxation degree of the arm's joints and muscle based on the tasks, so that the arm's impedance cannot generate unexpected energy but only dissipate the energy. This is what happens every time a human interacts with a robot through touch – the human does not take any action to destabilize the robot. The human keeps the system stable by modulating his/her hand impedance, which is related to the excess of passivity of the hand.

III. Main Results

The WMR's bilateral tele-driving system under a constant time-delay can be modeled as Fig. 2(a). MCU encompasses the master and its controller. SCU consists of the slave and its controller. HT is the human termination, ET is the environment termination, and CC is the communication channel. The signals in Fig. 2(a) will be defined later. In order to design a stabilizing controller for this teleoperation system, the potentially non-passive ET and the time delay existing in the communication channel need to be taken into account. Below, three different approaches to stabilization and stability analysis are presented.

By the above-described passivity analysis of the ET in (4), the WMR bilateral tele-driving system with an active ET can be described as in Fig. 2(b). The "WMR Tele-driving System" block encompasses the MSU, the SCU, and the CC. Outside the dashed box reside the human impedance augmented with the position-to-velocity mapping, which is assumed passive, as well as the passive component of the environment termination. The part of the ET's impedance inside the dashed box is active, since the ET may show an SOP of ε_e based on (4) ($\varepsilon_e=-0.5\dot{S}_L$), which is included and designed in the teleoperation system's model.

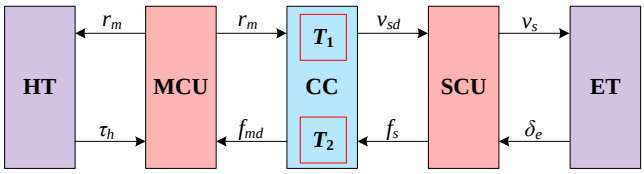

(a) Scheme of WMR's bilateral teleoperation under constant time-delay.

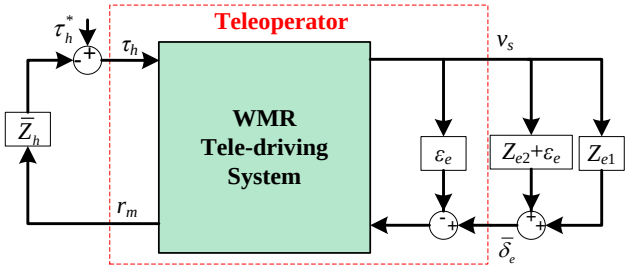

(b) WMR's tele-driving system with passivity compensation.

Fig. 2. WMR's tele-driving system with constant time-delay.

In this paper, for the proposed bilateral tele-driving system with the master robot (6) and the slave robot (3), its impedance matrix of the two-port network inside the dashed box in Fig. 2(b) can be modeled as

$$\begin{bmatrix}\tau_h\\ \bar{\delta}_e\end{bmatrix}=\begin{bmatrix}Z_{11} & Z_{12}\\ Z_{21} & Z_{22}\end{bmatrix}\begin{bmatrix}r_m\\ -v_s\end{bmatrix}, \tag{7}$$

where $\bar{\delta}_e=\delta_e+\varepsilon_e v_s$.

A. Method I: Llewellyn's criterion without compensation for the communication time delay

The two PD-like controllers for the master and the slave robots in Fig. 3(a) are designed as

$$\begin{cases}u_s(t)=\underbrace{C_s\left(r_m(t-T_1)-v_s(t)\right)}_{\text{P-Controller}}-\underbrace{K_s v_s(t)}_{\text{D-Controller}}\\ \bar{\tau}_m=\overbrace{-C_m\left(r_m(t-T_1-T_2)-v_s(t-T_2)\right)}^{\text{P-Controller}}-\overbrace{K_m r_m(t)}^{\text{D-Controller}}\end{cases}. \tag{8}$$

The above control laws are inspired by damping-injection control used for delay compensation in nonlinear teleoperation system [25] but have the following difference. The P term

involves the difference between the master and slave positions as it needs to be driven to zero. The D term is meant to dissipate energy typically involves the robot's velocity. In the WMR bilateral tele-driving system, the coordination is desired to happen between r_m and v_s. Thus, the P term in (8) is designed based on this coordination. Also, the D term in the slave controller involves the slave robot's velocity, but that in the master controller involves r_m.

For the two-port network of the teleoperator shown in Fig. 3(a), its impedance matrix can be written as

$$\begin{bmatrix} \tau_h \\ \bar{\delta}_e \end{bmatrix} = \begin{bmatrix} \bar{M}_m s + C_m e^{-(T_1+T_2)s} + K_m & C_m e^{-T_2 s} \\ C_s e^{-T_1 s} & s + C_s + K_s - \varepsilon_e \end{bmatrix} \begin{bmatrix} r_m \\ -v_s \end{bmatrix}. \quad (9)$$

In order to maintain the bilateral tele-driving system's stability, according to **Lemma 1**(see Appendix), the following conditions should be met:

$$\begin{aligned} &\mathrm{Re}(z_{11}) = K_m + C_m \cos(T_1\omega + T_2\omega) \geq 0 \\ &\mathrm{Re}(z_{22}) = K_s + C_s - \varepsilon_e \geq 0 \\ &2\,\mathrm{Re}(Z_{11})\left(\mathrm{Re}(Z_{22}) - \varepsilon_e\right) - \mathrm{Re}(Z_{12}Z_{21}) - \left|Z_{12}Z_{21}\right| . \\ &= 2\left(C_m \cos(T_1\omega + T_2\omega) + K_m\right)\left(C_s + K_s - \varepsilon_e\right) - \\ &C_s C_m \cos(T_1\omega + T_2\omega) - C_s C_m \geq 0 \end{aligned} \quad (10)$$

By simplifying (10), the following conditions are obtained:

$$\begin{aligned} &K_m \geq C_m \\ &K_s \geq \varepsilon_e \\ &C_m,\ C_s > 0 \end{aligned} . \quad (11)$$

From the stability conditions (10), non-zero communication time delays (T_1 and T_2) directly affects the stability condition and makes it more restrictive. Therefore, we then propose the second method described below to try to eliminate the time delay's influence on the absolute stability conditions by using wave transformations.

B. Method II: Llewellyn's criterion + wave transformation

In a teleoperation system, the time delay existing in the communication channel is a source of non-passivity in the system, which can cause instability. To compensate for it, the wave transformation has been widely used in the bilateral teleoperation literature. Through presenting a modification or extension to the communication channel using wave variables, from the perspective of passivity, wave transformation creates robustness to arbitrary time delays [11]. Here, the wave transformation is employed to eliminate the non-passivity caused by the time delay in the communication channel (Fig. 3(b)) and then **Lemma 1** is used to guarantee the stability of the overall system.

As [16] presents, the wave transformations for the two sides of the communication channel are implemented as

$$\begin{cases} U_m(t) = \frac{1}{\sqrt{2b}}\left(f_{md}(t) + b r_m(t)\right) \\ V_s(t) = \frac{1}{\sqrt{2b}}\left(-f_s(t) + b v_{sd}(t)\right) \end{cases}, \quad (12)$$

$$\begin{cases} U_s(t) = U_m(t - T_1) \\ V_m(t) = V_s(t - T_2) \end{cases}. \quad (13)$$

Combining (12) and (13), we can get the inputs and outputs of the two-port network representing the communication channel including the wave transformation as

$$\begin{cases} f_{md}(t) = \sqrt{\frac{b}{2}}\left(U_m(t) - V_m(t)\right),\ r_m(t) = \frac{U_m(t) + V_m(t)}{\sqrt{2b}} \\ f_s(t) = \sqrt{\frac{b}{2}}\left(U_s(t) - V_s(t)\right), v_{sd}(t) = \frac{U_s(t) + V_s(t)}{\sqrt{2b}} \end{cases}. \quad (14)$$

Combining (13) and (14), it is easy to prove that the two-port network representing the communication channel (with an initial energy of zero) is passive:

$$\begin{aligned} &E(t) = \int_0^t \left(f_{md}(\tau) r_m(\tau) - f_s(\tau) v_{sd}(\tau)\right) d\tau \\ &= \frac{1}{2}\int_0^t \left(U_m^T U_m - V_m^T V_m - U_s^T U_s + V_s^T V_s\right) d\tau \\ &= \frac{1}{2}\left(\int_{t-T_1}^t U_m^T U_m d\tau + \int_{t-T_2}^t V_s^T V_s d\tau\right) \geq 0 \end{aligned} . \quad (15)$$

We can also obtain (16) by combining (12), (13) and (14):

$$\begin{cases} f_{md}(t) = f_s(t - T_2) + b\left(r_m(t) - v_{sd}(t - T_2)\right) \\ v_{sd}(t) = r_m(t - T_1) + \frac{1}{b}\left(f_{md}(t - T_1) - f_s(t)\right) \end{cases}. \quad (16)$$

where the feedback force from the slave robot is the force caused by the difference between the desired velocity and actual velocity, $f_s(t) = C_m\left(v_{sd}(t) - v_s(t)\right)$. The controllers for the master and slave robots are designed as

$$\begin{cases} u_s(t) = C_s\left(v_{sd}(t) - v_s(t)\right) - K_s v_s(t) \\ \tau_m(t) = -f_{md}(t) - K_m r_m(t) \end{cases}. \quad (17)$$

With the wave transformation, the communication channel is passive as shown in (15). Then, we employ **Lemma 1** below to design the whole bilateral teleoperation system. Combining (16) and (17), the impedance matrix of the teleoperation system in Fig. 3(b) can be written as

$$\begin{bmatrix} \tau_h \\ \bar{\delta}_e \end{bmatrix} = \begin{bmatrix} M_m s + K_m + Z_{mm} & Z_{ms} \\ Z_{sm} & M_s s + K_s - \varepsilon_e + Z_{ss} \end{bmatrix} \begin{bmatrix} r_m \\ -v_s \end{bmatrix}, \quad (18)$$

where

$$\begin{aligned} &Z_{mm} = \frac{C_m e^{-(T_1+T_2)s} + b + C_m - b e^{-(T_1+T_2)s}}{Z_{sd}},\ Z_{ms} = \frac{2C_m e^{-T_2 s}}{Z_{sd}}, \\ &Z_{sm} = \frac{2C_s e^{-T_1 s}}{Z_{sd}},\ Z_{ss} = \frac{C_s\left(1 + e^{-(T_1+T_2)s}\right)}{Z_{sd}}, \\ &Z_{sd} = 1 - \frac{C_m}{b} e^{-(T_1+T_2)s} + e^{-(T_1+T_2)s} + \frac{C_m}{b}. \end{aligned}$$

According to **Lemma 1**, to maintain the absolute stability of (18), the following conditions should be met:

$$\begin{aligned}
&\mathrm{Re}(Z_{11}) = \frac{2b^2 C_m}{\left(b^2 + C_m{}^2\right) + \left(b^2 - C_m{}^2\right)\cos\left(\left(T_1 + T_2\right)\omega\right)} + K_m \geq 0;\\
&\mathrm{Re}(Z_{22}) = \frac{b^2 C_s\left(1 + \cos\left(\left(T_1 + T_2\right)\omega\right)\right)}{\left(b^2 + C_m{}^2\right) + \left(b^2 - C_m{}^2\right)\cos\left(\left(T_1 + T_2\right)\omega\right)} + K_s - \varepsilon_e \geq 0; \qquad (19)\\
&2\,\mathrm{Re}(Z_{11})\mathrm{Re}(Z_{22}) - \mathrm{Re}(Z_{12}Z_{21}) - \left|Z_{12}Z_{21}\right|\\
&= 2\,\mathrm{Re}(Z_{11})\mathrm{Re}(Z_{22}) - \frac{8C_m C_s b^4 \cos^2\left(\dfrac{\left(T_1 + T_2\right)\omega}{2}\right)}{\left[\left(b^2 + C_m{}^2\right) + \left(b^2 - C_m{}^2\right)\cos\left(\left(T_1 + T_2\right)\omega\right)\right]^2} \geq 0.
\end{aligned}$$

By simplification of the above conditions, the absolute stability conditions for (18) are

$$\begin{aligned}
&K_m \geq 0\\
&K_s \geq \varepsilon_e \qquad .\\
&C_m,\ C_s > 0
\end{aligned} \qquad (20)$$

A comparison between the conditions (11) and (20) shows that the wave transformation eliminates the influence of the time delay on the absolute stability conditions. In the first two conditions in (20), the denominator is always positive for any value of T_1 and T_2 and the same is true for the numerator of the second condition. This means that employing wave transformations have alleviated the adverse influence of time delay on the stability.

C. Method III: Passivity analysis + wave transformation

Method II can give an absolute stability condition, but lots of computation is introduced to the impedance matrix (18) due to the presence of the wave transformations. A more direct but more conservative method is to guarantee the passivity of each of the HT, MCU, CC, SCU and ET such that the end-to-end WMR's bilateral tele-driving system will be passive and therefore stable. Equation (15) proved that the communication channel with the wave transformation is passive. The controllers for the master and slave robots as designed in (17) for Method II are again used here. In order to guarantee the passivity of the MCU and SCU, the controller parameters are designed via the following process.

1) MCU and HT

HT is assumed to be passive [31] in this paper. The MCU can be simplified as a one-port network in Fig. 3(c).

The input-output relationship for this one-port network is

$$\tau_h + f_{md} = Z_{MCU} r_m, \qquad (21)$$

where $Z_{MCU} = \bar{M}_m s + K_m$.

To make this network passive, we need to design the controller of the master robot so that

$$\mathrm{Re}\left(Z_{MCU}\right) = K_m \geq 0. \qquad (22)$$

2) SCU and Modified ET

As the analysis in Sec. II, the ET is potentially non-passive, and we have decomposed the ET into a passive part and an active part. Since we have included the potential active part of the ET into the SCU to design the related controllers, the modified ET shown in Fig. 3(d) is passive, which is easy to prove based on (4) because ε_e corresponds to the worst case of the ET. The SCU can be described as a two-port network shown inside the left dashed box in Fig. 3(d). The modified ET can be described as the one-port network shown inside the right dashed box in Fig. 3(d).

Then, the transfer function of the SCU two-port network can be described as

$$\begin{bmatrix} -v_s \\ v_{sd} \end{bmatrix} = \frac{1}{s + K_s - \varepsilon_e}\begin{bmatrix} 1 & -\dfrac{C_s}{C_m} \\ -1 & \dfrac{s + C_s + K_s - \varepsilon_e}{C_m} \end{bmatrix}\begin{bmatrix} \bar{\delta}_e \\ f_s \end{bmatrix} = Z_{SCU}\begin{bmatrix} \bar{\delta}_e \\ f_s \end{bmatrix}. \qquad (23)$$

To make this two-port network passive, by **Lemma 2** (see Appendix), we need to design Z_{SCU} to be positive real. Therefore, by **Definition 1** (see Appendix), (23) should meet the following conditions:

(1) Poles of all elements of $Z_{SCU}(s)$ are in $\mathrm{Re}[s] \leq 0$, requiring

$$\mathrm{Re}(poles) = -\left(K_s - \varepsilon_e\right) \leq 0. \qquad (24)$$

(2) For all real ω for which jω is not a pole of any element of $Z_{SCU}(s)$, the matrix $Z_{SCU}(j\omega) + Z_{SCU}^T(-j\omega)$ is positive semi-definite for all $\omega \in R$. We have

$$Z_{SCU}(j\omega) + Z_{SCU}^T(-j\omega) = \begin{bmatrix} \dfrac{2\left(K_s - \varepsilon_e\right)}{\left(K_s - \varepsilon_e\right)^2 + \omega^2} & \dfrac{j\omega\left(\dfrac{C_s}{C_m} - 1\right) - \left(K_s - \varepsilon_e\right)\left(\dfrac{C_s}{C_m} + 1\right)}{\left(K_s - \varepsilon_e\right)^2 + \omega^2} \\ \dfrac{-j\omega\left(\dfrac{C_s}{C_m} - 1\right) - \left(K_s - \varepsilon_e\right)\left(\dfrac{C_s}{C_m} + 1\right)}{\left(K_s - \varepsilon_e\right)^2 + \omega^2} & \dfrac{2\dfrac{\left(C_s + K_s - \varepsilon_e\right)\left(K_s - \varepsilon_e\right)}{C_m} + 2\dfrac{\omega^2}{C_m}}{\left(K_s - \varepsilon_e\right)^2 + \omega^2} \end{bmatrix},$$

which is positive semi-definite if its leading principal minors are all non-negative:

1st-order principal minor:

$$2\left(K_s - \varepsilon_e\right) \geq 0; \qquad (25)$$

2nd-order principal minor:

$$\begin{aligned}
&\left(\frac{4\left(K_s - \varepsilon_e\right)}{C_m} - \left(\frac{C_s}{C_m} - 1\right)^2\right)\omega^2 +\\
&\left(\frac{4\left(C_s + K_s - \varepsilon_e\right)\left(K_s - \varepsilon_e\right)^2}{C_m} - \left(K_s - \varepsilon_e\right)^2\left(\frac{C_s}{C_m} + 1\right)^2\right) \geq 0
\end{aligned} \qquad . \qquad (26)$$

By solving the conditions (24)-(26), the following conditions are obtained:

$$\begin{aligned}
&K_s \geq \varepsilon_e\\
&C_m,\ C_s > 0 \qquad .\\
&\frac{4\left(K_s - \varepsilon_e\right)}{C_m} \geq \left(\frac{C_s}{C_m} - 1\right)^2
\end{aligned} \qquad (27)$$

Table 1 gives the comparison of the above three methods. From this table, it can be seen that Method I needs the

teleoperator's controller to compensate for the time-delay's non-passivity, and the stability conditions are conservative owing to the time-delay. With the wave transformation to compensate for the time-delay, comparing Methods II and III, we found that Method II is less conservative but involves lengthier calculations. Method III is more direct and easier but results in conservative stability conditions.

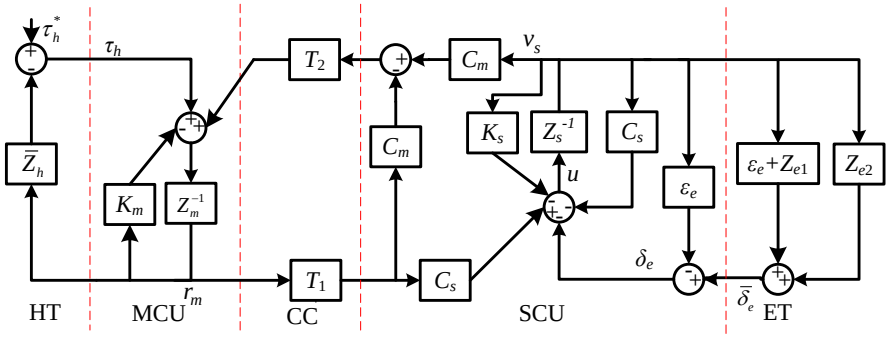

(a) Bilateral tele-driving control of WMR with controllers (16).

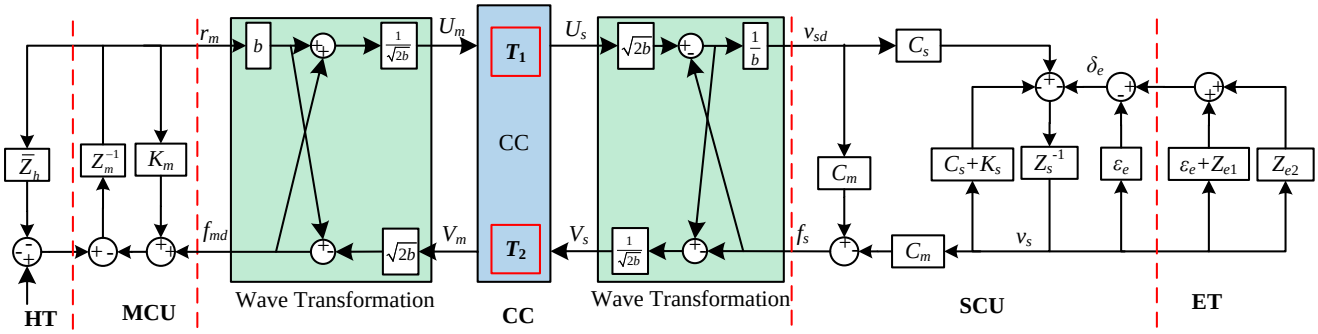

(b) WMR's bilateral tele-driving scheme with wave transformation.

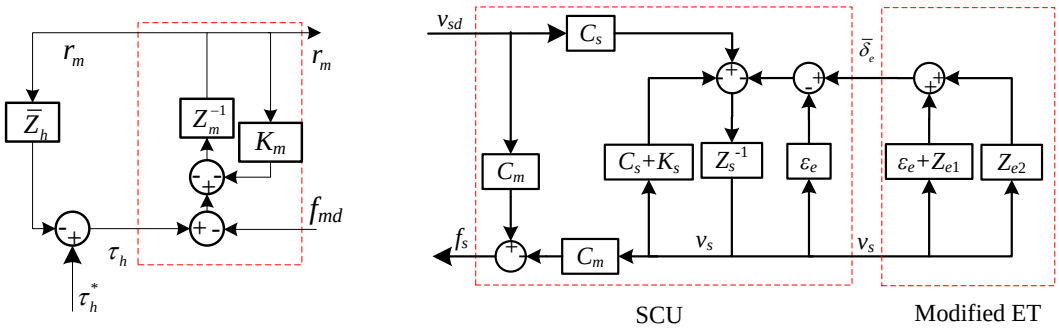

(c) Network of MCU and HT.

(d) Network of SCU and ET.

Fig. 3. Controller design of WMR tele-driving system with time-delay.

TABLE 1 Comparison of these three methods.

Method	Compensation for time delay's non-passivity	Compensation for ET's non-passivity	Teleoperation stability analysis approach	Complexity of design	Stability condition
I	By controller design	Including it into the teleoperator	Llewellyn's criterion	Less	Conservative
II	By wave transformations	Including it into the teleoperator	Llewellyn's criterion	More	Less conservative
III	By wave transformations	Including it into the teleoperator	Passivity guarantee	Less	Conservative

IV. Case Studies

In the following experimental cases, the bilateral tele-driving of a virtual WMR on a soft terrain with slippage is considered under constant communication time-delay. Overwhelming literatures show that the wheel's slippage is influenced mainly by soil's mechanical parameters (e.g., friction angle) [26] and the terrain's geometric parameters (e.g., slope angle). In this section, a virtual terrain that can give rise to a certain shortage of passivity is created as the environment termination, and a series of semi-physical experiments is done to validate the proposed methods of the WMR bilateral tele-driving under longitudinal slippage and constant time-delay.

A. Experimental Setup

To validate the theoretical findings in this paper, following experiments are done with a Phantom Premium 1.5A haptic device (as the master robot) and ROSTDyn (as the slave robot).

1) Master Robot and Human Operator

In our WMR's tele-driving experimental system (Fig. 4(a)), the master robot is a Phantom Premium 1.5A haptic device (Geomagic Inc., Wilmington, MA, USA) (Fig. 4(b)), and the slave robot (WMR) is a WMR's dynamic simulation platform specially for a soft terrain named ROSTDyn which was developed by the authors [27], and the communication channel between the master site and the slave site is implemented by using a local area network (LAN). As the WMR only travels straightly, the first joint q_1 of the Phantom is used as the commands and the other two joints are locked by a high gain position controller (q_2=q_3=0). Based on the works in [28], the Phantom's inertia is M_m=0.0035kg·m^2. In (6), λ=0.1 and B_{Lv}=-0.035kg·m^2·s^{-1}.

In the following experiments, based on (6), the torque acting on the Phantom from the human operator can be estimated as

$$\tau_h = \bar{M}_m \dot{r}_m - \bar{\tau}_m . \tag{28}$$

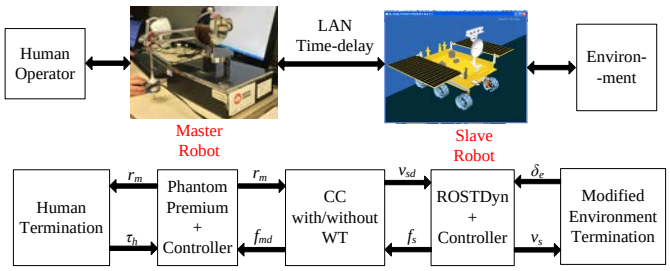

(a) Experimental scheme of WMR bilateral tele-driving system.

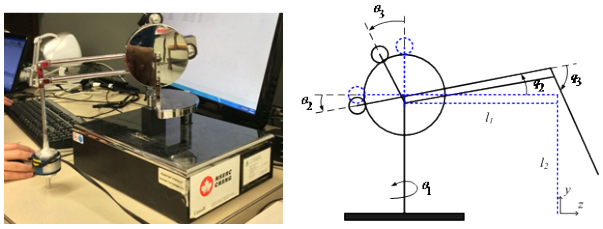

(b) The master Phantom 1.5A robot.

Fig. 4. Experiment platform setup of WMR bilateral tele-driving system.

2) Slave Robot and Environment

In our experimental system, ROSTDyn is used as the slave robot, which is developed based on Vortex software (CMLabs, Montreal, Canada) and the wheel-terrain interaction model on the soft terrains. ROSTDyn can realize a real-time simulation with good fidelity [27]. In this simulation platform, the wheel's slippage fidelity has been validated by experiments, so it can be used for simulating a slave WMR with slippage. The terramechanics model between the wheel and the terrain used in ROSTDyn is given as:

$$\begin{cases} F_{\mathrm{N}} = rb\sigma_m A + rb\tau_m B = AX + BY \\ F_{\mathrm{DP}} = rb\tau_m A - rb\sigma_m B = AY - BX \\ M_{\mathrm{R}} = r^2 b(\theta_1 - \theta_2)\tau_m / 2 = rCY \end{cases}, \tag{29}$$

where $A = \dfrac{\cos\theta_m - \cos\theta_2}{\theta_m - \theta_2} + \dfrac{\cos\theta_m - \cos\theta_1}{\theta_1 - \theta_m}$;

$B = \dfrac{\sin\theta_m - \sin\theta_2}{\theta_m - \theta_2} + \dfrac{\sin\theta_m - \sin\theta_1}{\theta_1 - \theta_m}$; $C = (\theta_1 - \theta_2)/2$;

$X = rb\sigma_m$; $Y = rb\tau_m$;

$\tau_m = E(c + \sigma_m \tan\varphi)$; $\sigma_m = K_s r^N (\cos\theta_m - \cos\theta_1)^N$;

$E = 1 - \exp\{-r[(\theta_1 - \theta_m) - (1-s)(\sin\theta_1 - \sin\theta_m)]/K\}$;

$K_{\mathrm{S}} = K_c / b + K_\varphi$; $N = n_0 + n_1 s$.

In (29), F_N is the normal force, F_{DP} is the drawbar pull force, and M_R is the moment generated by the interaction between the wheel and the terrain, s is the wheel's slippage and φ is the internal friction angle, which is decided by the terrain's characteristics in practice. The other parameters are defined in [27]. Different from the kinematic model (3) of the WMR, this model describes a dynamic interaction between the wheel and the terrain, which models the interaction force/torque influenced by the slippage.

The terrain has a slope with an angle of 15°, and its size is 10m (x)×10m (y). The most sensitive parameter φ in (29) to the wheel's slippage [29] is set as a position-varying function. The following parameters can induce the terrain physically become harder as the WMR moves forward:

$$\varphi = \begin{cases} 1.35 & (8.1 \le x < 10) \\ 0.6 + 0.15(x - 3.1) & (3.1 \le x < 8.1) \\ 0.6 & (0 < x < 3.1) \end{cases}. \tag{30}$$

Here, x is the WMR's position. While climbing a sloped terrain, the bigger the φ is, the smaller the slippage is, so that a negative $\dot{S}$ appears while S is positive, which can then make the ET potentially non-passive. In addition, as (3) shows, the output force of the environment termination is varying due to the fact that the slippage varies and the WMR's states change.

In addition, the time delay is implemented by using a software buffer. The forward time delay is set at 2s and the backward time delay is set at 3s. For the wave transformation, the parameter b in Fig. 3(b) is set at 1 considering the tasks of the slave robot and the environment. In the experiments, the energy of the environment termination is calculated based on its input v_s and output δ_e.

B. Experiments with Method I

To validate Method I, the controller parameters are set to be

Case I: $C_m = 15$, $C_s = 10$, $K_m = 3$, $K_s = 0.0$ (violating (11));

Case II: $C_m = 10$, $C_s = 10$, $K_m = 10.5$, $K_s = 1.0$ (meeting (11)).

The experimental results are shown in Fig. 5 (Case I) and Fig. 6 (Case II). The position-velocity plots of the experiments in Case I (Fig. 5(a)) (such a scenario may be encountered in an unknown terrain) show that the teleoperation system with Case I is unstable (fast fluctuations), which is to be expected since Case I violates the stability conditions (11). As Fig. 5(c) shows, the ET is non-passive due to the slippage shown in Fig. 5(b). In Case I, the CC's non-passivity can also cause the system's instability, which was predicted in Sec. III. Obviously, in this case, the operator cannot maintain the position-velocity coordination well, and fully loses the control to the slave WMR instead of feeling a fluctuating feedback force (Fig. 5(d)).

With Case II (such a scenario will be encountered in a known terrain, and the slippage can be tested or estimated), the ET's non-passivity has been fully compensated for (Fig. 6(c)). In

Case II, the controller parameters satisfy (11), resulting in a stable system (Fig. 6(a)). Note that it was reasonable to set K_s (and ε_e) at 1.0 based on Fig. 6(b) and the calculation of $\varepsilon_e = -0.5\dot{S}_L$. The position-velocity coordination is tracked with each other well (Fig. 6(a)), which means that the human operator can control the slave's velocity by the commands at a desired level. Note that the force tracking performance (Fig. 6(d)) is undermined by the D-term, which was used to ensure stability despite time delays.

From the above results, we can obtained:

(1) The communication time-delay will induce the system's instability, which can be effectively compensated for by the designed D controller.

(2) The ET's non-passivity is also one unstable factor for the system, which can be eliminated by its SOP.

(3) The conditions given by Method I are conservative and transparency is poor due to the conservative D-term.

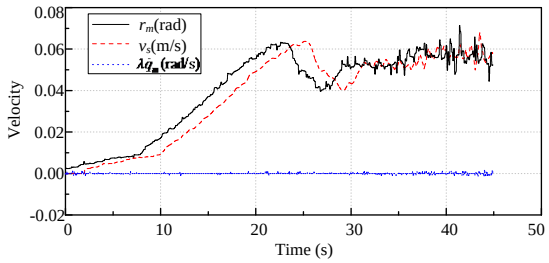

(a) Position-velocity coordination.

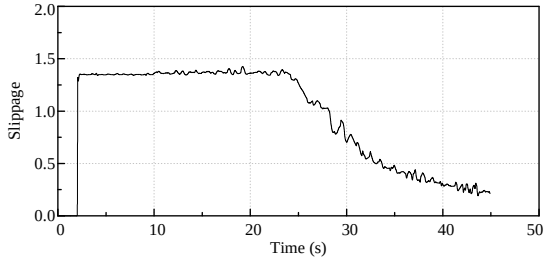

(b) Terrain/WMR slippage.

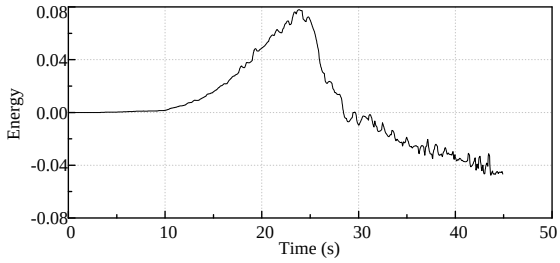

(c) Energy generated by ET.

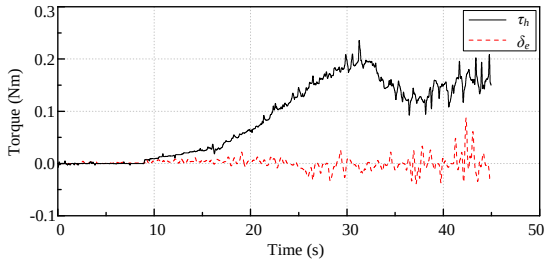

(d) Force tracking performance.

Fig. 5. Experiment results with Case I.

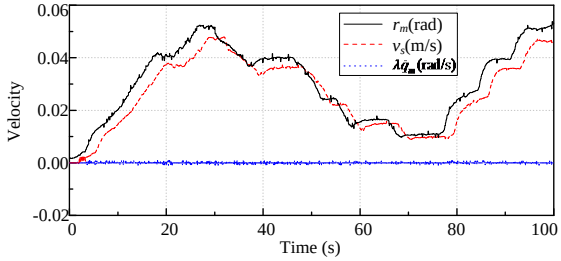

(a) Position-velocity coordination.

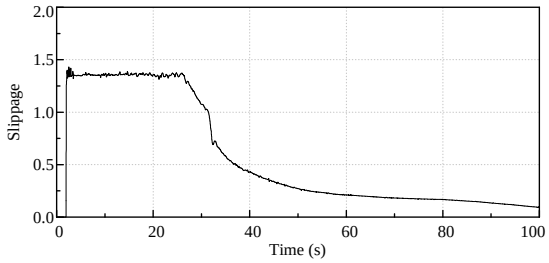

(b) WMR/Terrain slippage.

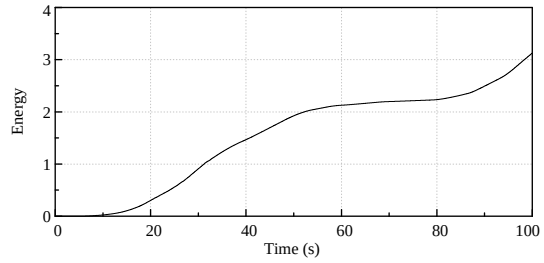

(c) Energy generated by the modified ET.

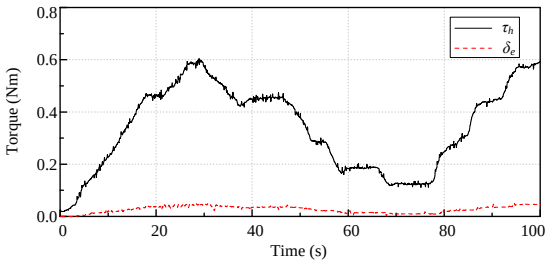

(d) Force tracking performance.

Fig. 6. Experiment results with Case II.

C. *Experiments with Method II and Method III*

In the experiments of the WMR bilateral tele-driving with wave transformation to validate the stability conditions obtained by Method II and III, a set of the controller parameters are designed:

Case I: $C_m = 10$, $C_s = 10$, $K_s = 0.0$ (violating the stability conditions of Method II or Method III);

Case II: $C_m = 10$, $C_s = 10$, $K_s = 1.0$ (meeting the stability conditions of Method II and Method III);

Case II: $C_m = 10$, $C_s = 15$, $K_s = 1.0$ (meeting the stability conditions of Method II, but not for Method III).

Note that the stability conditions of Method II are given by (20) while those for Method III are given by (27).

The experiment results are shown in Fig. 7-9. The position-velocity plots of the experiments in Case I (Fig. 7(a)) (such a scenario may be encountered in an unknown terrain while time-delay is known) show that the teleoperation system with Case I is unstable, since Case I violates the stability conditions of Method II and III. As Fig. 7(c) shows, the ET is

non-passive due to the slippage profile of Fig. 7(b). As a result, the position-velocity coordination is not tracked well and the operator cannot tele-drive the slave WMR on a desired level while he/she feels a fluctuating feedback force (Fig. 7(d)).

With Case II (such a scenario may be encountered in a known terrain while passivity and Llewellyn's criterion are considered at the same time), the termination's non-passivity is fully compensated for by the modified ET (Fig. 8(c)), and the controller parameters are within the stability conditions of Methods II and III, which results in a stable tele-driving system (Fig. 8(a) shows the results for both Methods II and III; note that these are two different stability analysis methods for the same control laws (17)). Note that it was reasonable to set K_s (and ε_e) at 1.0 based on Fig. 8(b) and the calculation of $\varepsilon_e = -0.5\dot{S}_L$. The slave's velocity tracks with the master's position well (Fig. 8(a)), which means that the human operator can tele-drive the slave's velocity under the proposed scheme. The force tracking performance is also good as Fig. 8(d) shows.

With Case III (such a scenario may be encountered in a known terrain while only Llewellyn's criterion is considered), the experiment results (Fig. 9) are similar with the Case II. This shows that Method III is more conservative than Method II. Note that the controllers chosen in Case III met the stability conditions of Method II but not those for Method III.

From the above results, the following conclusions are obtained:

(1) The wave transformation is effective to compensate for the time-delay.

(2) The conditions given by Method III are more conservative than that obtained from Method II.

(3) The force transparency is improved comparing with Method I, which means the human operator can feel the environment correctly ($\tau_h \approx \delta_e$), while it is limited by the D-term for the stability in Method I.

Besides of the above experiments, some sets of different controller parameters and different slippage parameters were also studied to validate the proposed controllers. In all experiments, it was found that under the proposed stability conditions, the WMR tele-driving system is stable while the performance may not always be ideal. Therefore, it is necessary to optimize the controller parameters for an ideal velocity tracking performance and force feedback transparency.

In summary, from the experiment results, it is seen that the proposed methods in this paper can be used to design a stable bilateral teleoperation system with non-passive terminals and a constant time delay. With the proposed controllers, as the experimental results show, the slave WMR can track the master commands well, and the experienced WMR's velocity loss associated with a traditional velocity controller caused by the wheel's slippage is effectively compensated for with the presented acceleration-level controller of the motor, as well the system's stability is guaranteed. However, since in this paper, the communication channel's non-passivity/instability is compensated for by a D-term controller or wave transformation as well as the ET's, the system's transparency will become not so ideal. On a measureable system, the time-domain passivity controller [33] may be a better choice, which will be researched in the future.

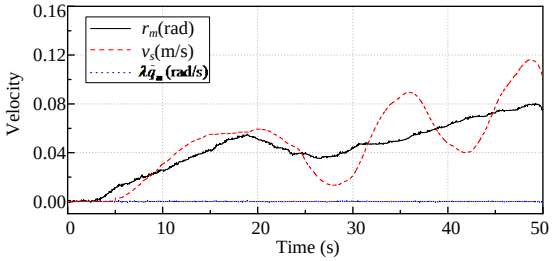

(a) Position-velocity coordination.

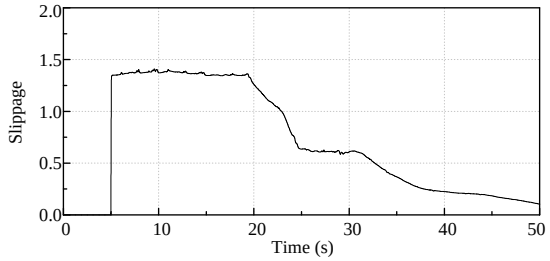

(b) WMR/Terrain slippage.

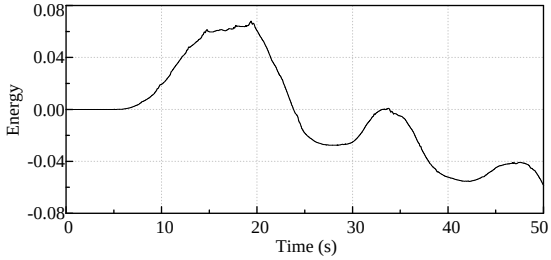

(c) Energy generated by the modified ET.

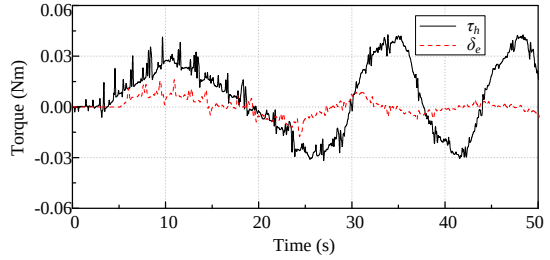

(d) Force tracking performance.

Fig. 7. Experiment results with Case I.

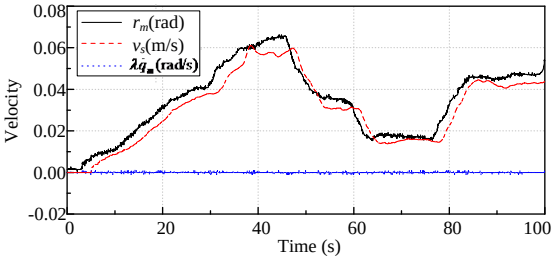

(a) Position-velocity coordination.

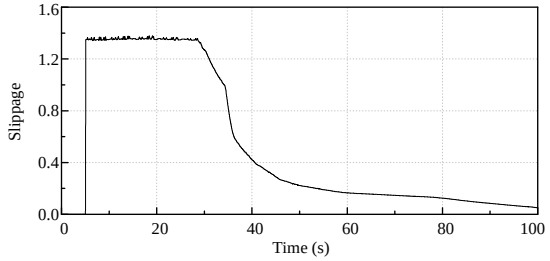

(b) WMR/Terrain slippage.

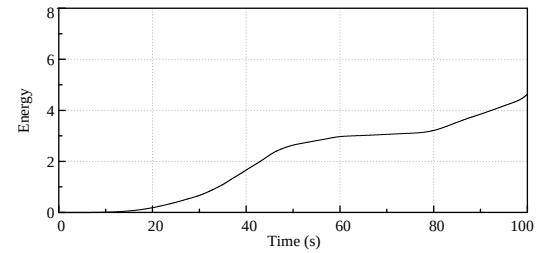

(c) Energy generated by the modified ET.

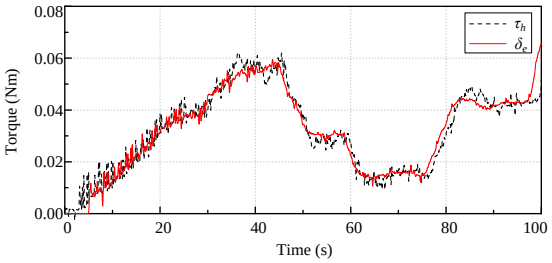

(d) Force tracking performance.

Fig. 8. Experiment results with Case II.

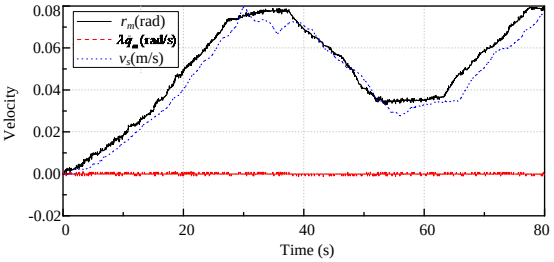

(a) Position-velocity coordination.

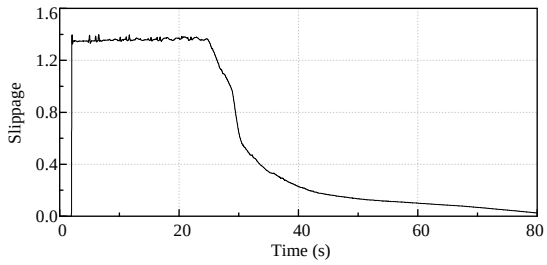

(b) WMR/Terrain slippage.

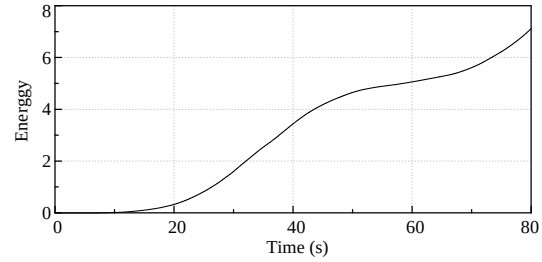

(c) Energy generated by the modified ET.

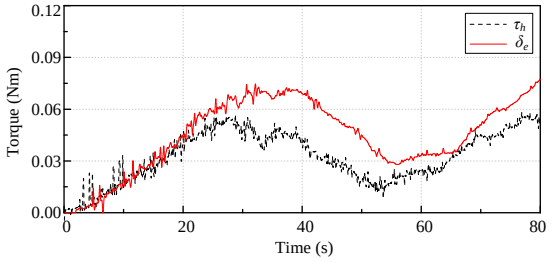

(d) Force tracking performance.

Fig. 9. Experiment results with Case III.

V. Conclusion

Three methods for haptic tele-driving control of a WMR with constant time delays and non-passive environment termination are proposed in this paper. In WMR tele-driving, we show that the WMR/terrain slippage may induce ET non-passivity. In such a tele-driving system, the WMR's (linear) velocity follows the master robot's position, and the force feedback felt by the human operator is related to the difference between the commanded velocity and the actual velocity of the WMR. We propose three methods to design the WMR's tele-driving system with the ET's non-passivity as well as the constant time delay thorough Llewellyn's criterion and a passivity-based criterion with and without the wave transformation. Another consideration in this work is that the WMR controller is a kinematic controller, which is the case for most of the available mobile robots. Lastly, the proposed methods are validated by a series of experiments.

In the future, considering a more practical tele-driving task, the influence of the WMR's rotation and the communication time-varying delays on its tele-driving will be researched. Additionally, although the position-velocity coordination is more effective to tele-drive a WMR, the position-position coordination should also be considered for a more precise task with challenging issues of non-holonomic constraint and wheel slippage.

Appendix

Lemma 1 (Llewellyn's criterion [24]) *The two-port network (7) is absolutely stable (i.e., the overall system is bounded-input/bounded output stable assuming the passivity of both terminations) if and only if*

(1) $Z_{11}(s)$ and $Z_{22}(s)$ have no poles in the right half plane;

(2) Any poles of $Z_{11}(s)$ and $Z_{22}(s)$ on the imaginary axis are simple with real and positive residues;

(3) For $s = j\omega$ and all real values of ω:

$$\mathrm{Re}(Z_{11}) \geq 0$$

$$\mathrm{Re}(Z_{22}) \geq 0$$

$$2\,\mathrm{Re}(Z_{11})\,\mathrm{Re}(Z_{22}) - \mathrm{Re}(Z_{12}Z_{21}) - \left|Z_{12}Z_{21}\right| \geq 0$$

.

Lemma 2 [30] *The LTI minimum realization*

$$\dot{x} = Ax + Bu$$

$$y = Cx + Du$$

with $G(s) = C(sI - A)^{-1}B + D$ *is*

(1) passive if $G(s)$ is positive real;

(2) *strictly passive if $G(s)$ is strictly positive real.*

Definition 1 [30] *An $n \times n$ proper rational transfer function matrix $G(s)$ is said to be positive real if*

(1) poles of all elements of $G(s)$ are in $\mathrm{Re}[s] \leq 0$;

(2) for all real ω for which $j\omega$ is not a pole of any element of $G(s)$, the matrix $G(j\omega) + G^T(-j\omega)$ is positive semi-definite, and

(3) any pure imaginary pole of $j\omega$ of any element of $G(s)$ is a simple pole and the residue matrix $\lim_{s \to j\omega}(s - j\omega)G(s)$ is positive semi-definite Hermitian.

REFERENCE

[1] L. Ding, H. Gao, Z. Deng, K. Yoshida, and K. Nagatani, "Experimental study and analysis on driving wheels' performance for planetary exploration rovers moving in deformable soil," *J. Terramech*, vol. 48, no. 1, pp. 27–45, Feb. 2011.

[2] G. Ishigami, K. Nagatani, and K. Yoshida, "Path following control with slip compensation on loose soil for exploration rover," in *Proc. IEEE/RSJ Int. Conf. Intell. Robots Syst.*, 2006, pp. 5552-5557.

[3] G. Reina, L. Ojeda, A. Milella, and J. Borenstein, "Wheel slippage and sinkage detection for planetary rovers," *IEEE/ASME Transactions on Mechatronics*, vol. 11, no. 2, pp. 185-195, Apr. 2006.

[4] L. Ding, K. Nagatani, K. Sato, et al, "Terramechanics-based high-fidelity dynamics simulation for wheeled mobile robot on deformable rough terrain," in *Proc. of IEEE Int. Conf. Robot. and Autom.*, 2010, pp. 4922–4927.

[5] Y. Tian and N. Sarkar, "Control of a mobile robot subject to wheel slip," *J. Intell. Robot Syst.*, vol. 74, no. 4, pp. 915-929, Jun. 2014.

[6] T. B. Sheridan, "Space teleoperation through time delay: review and prognosis," *IEEE Trans. Robot. Autom.*, vol. 9, no. 5, pp. 592–606, Oct. 1993.

[7] C. Yang, X. Wang, Z. Li, Y. Li and C. Su, "Teleoperation control based on combination of wave variable and neural networks," *IEEE Trans. Syst., Man, Cybern., Syst.*, vol. 47, no. 8, pp. 2125-2136, Aug. 2017.

[8] D. Wang , P. Huang and Z. Meng, "Coordinated stabilization of tumbling targets using tethered space manipulators," *IEEE Trans. Aerosp. Electr. Syst.*, vol. 51, no. 3, pp. 2420-2432, Jul. 2015.

[9] P. Huang , D. Wang , Z. Meng , F. Zhang and Z Liu, "Impact dynamic modelling and adaptive target capturing control for tethered space robots with uncertainties," *IEEE/ASME Trans. Mechatron.*, vol.21, no.5, pp.2260-2271, Oct. 2016.

[10] F. Zhang and P. Huang, "Dynamics and stability control of maneuverable tethered space net," *IEEE/ASME Trans. Mechatron.*, vol. 22, no. 2, pp. 983-993, Apr. 2017.

[11] T. Imaida, Y. Yokokohji, T. Doi, M. Oda and T. Yoshikawa, "Ground -space bilateral teleoperation of ETS-VII robot arm by direct bilateral coupling under 7-s time delay condition," *IEEE Trans. Robot. Automat.*, vol. 20, no. 3, pp. 499-511, Jun. 2004.

[12] W. K. Yoon, T. Goshozono, H. Kawabe, et al, "Model-based space robot teleoperation of ETS-VII manipulator," *IEEE Trans. Robot. Automat.*, vol. 20, no. 3, pp. 602-612, Jun. 2004.

[13] X. Yang, C. Hua, J. Yan and X. Guan, "An exact stability condition for bilateral teleoperation with delayed communication channel," *IEEE Trans. Syst., Man, Cybern., Syst.*, vol. 46, no. 3, pp. 434-439, Mar. 2016.

[14] R.J. Anderson and M.W. Spong, "Asymptotic stability for force reflecting teleoperators with time delay," *Int. J. Robot. Res.*, vol. 11, no. 2, pp. 135-149, Apr. 1992.

[15] G. Niemeyer and J. J. E. Slotine, "Stable adaptive teleoperation," *IEEE Journal of Oceanic Engineering*, vol. 16, no. 1, pp. 152–162, Jan. 1991.

[16] G. Niemeyer and J. E. Slotine, "Telemanipulation with time delays," *Int. J. Robot. Res.*, vol. 23, no. 9, pp. 873–890, Sep. 2004.

[17] D. Lee, O. M. Palafox and M. W. Spong, "Bilateral teleoperation of a wheeled mobile robot over delayed communication network," in *Proc. IEEE Int. Conf. Robot. Autom.*, 2006, pp. 3298-3303.

[18] E. Slawinski, V. A. Mut, P. Fiorini and L. R. Salinas, "Quantitative absolute transparency for bilateral teleoperation of mobile robots," *IEEE Trans. Sys. Man & Cybern. Part A: Sys. & Hum.*, vol. 42, no. 2, pp. 430-442, Mar. 2012.

[19] J. Ware and Y.-J. Pan, "Realisation of a bilaterally teleoperated robotic vehicle platform with passivity control," *IET Control Theory Appl.*, vol. 5, no. 8, pp. 952-962, May 2011.

[20] H. V. Quang, I. Farkhatdinov and J. H. Ryu, "Passivity of delayed bilateral teleoperation of mobile robots with ambiguous causalities: Time domain passivity approach," in *Proc. IEEE/RSJ Int. Conf. Intell. Robots Syst.*, 2012, pp. 2635-2640.

[21] P. Malysz and S. Sirouspour, "A task-space weighting matrix approach to semi-autonomous teleoperation control," in *Proc. IEEE/RSJ Int. Conf. Intell. Robots Syst.*, 2011, pp. 645-652.

[22] W. Li, L. Ding, H. Gao and M. Tavakoli, "Kinematic bilateral teleoperation of wheeled mobile robots subject to longitudinal slippage," *IET Control Theory & Applications*, vol. 10, no. 2, pp.111-118, Jan. 2016.

[23] W. Li, L. Ding, Z. Liu, W. Wang, H. Gao and M. Tavakoli, "Kinematic bilateral tele-driving of wheeled mobile robots coupled with slippage," *IEEE Trans. Ind. Electron.*, vol. 64, no. 3, pp. 2147-2157, Mar. 2017.

[24] S. Haykin, Active Network Theory. Addison-Wesley, 1970.

[25] E. Nuno, R. Ortega, N. Barabanov and L. Basanez, "A globally stable PD controller for bilateral teleoperators," *IEEE Trans. Robot.*, vol. 24, no. 3, pp. 753-758, Jun. 2008.

[26] The Rover Team, "Characterization of the Martian surface deposits by the Mars Pathfinder Rover, Sojourner," *Science*, vol. 278, no. 5344, pp. 1765-1768, Dec. 1997.

[27] W. Li, L. Ding, H. Gao, Z. Deng and N. Li, "ROSTDyn: Rover simulation based on terramechanics and dynamics," *J. Terramech.*, vol. 50, pp. 199-210, 2013.

[28] M.C. Cavusoglu, D. Feygin and F. Tendick, "A critical study of the mechanical and electrical properties of the PHANToM haptic interface and improvements for high performance control," *Presence: Teleoperators & Virtual Environments*, vol. 11, no. 6, pp. 555-568, Oct. 2002.

[29] W. Li, Z. Liu, H. Gao, L. Ding, N. Li and Z. Deng, "Soil parameter modification used for boosting predictive fidelity of planetary rover's slippage," *J. Terramech.*, vol. 56, pp. 173-184, 2014.

[30] H. Khalil, Nonlinear Systems. Prentice Hall, 2002.

[31] M. Tavakoli, A. Aziminejad, R. V. Patel, and M. Moallem, "High-fidelity bilateral teleoperation systems and the effect of multimodal haptics," *IEEE Trans. Syst. Man Cybern.-Part B*, vol. 37, no. 6, pp. 1512-1528, Dec. 2007.

[32] R. Lozano, B. Maschke, B. Brogliato and O. Egeland, Dissipative systems analysis and control: theory and applications. Secaucus: Springer-Verlag New York, 2007.

[33] J. Ryu, D. Kwon and B. Hannaford, "Stable Teleoperation with Time-Domain Passivity Control," *IEEE Trans. Robot. Automat.*, vol. 20, no. 2, pp. 365–373, Apr. 2004.

[34] R. Tao, M. Tavakoli, "Multilateral haptic system stability analysis: The effect of activity or passivity of terminations via a series-shunt approach," in *IEEE Haptics Symposium*, 2014, pp. 203-208.